

## International Journal of Strategic Management and Economic Studies (IJSMES)

ISSN: 2791-299X

# Spatial distribution and structural characteristics of Imorona-Itsindro suite in Ambatofinandrahana district, Madagascar

### RANAIVOSON Nirina Tedy¹, RASOAMALALA Vololonirina¹, RAZANANIRINA Henri Délice²

<sup>1</sup>Doctoral school of Earth Sciences and Evolution, Faculty of Sciences, University of
Antananarivo, Madagascar

<sup>2</sup>Ministry of Mines, Madagascar

Abstract: The principal aim of this study is to map the lithology of the Imorona-Itsindro suite and to constrain the tectonic framework of the Ambatofinandrahana district in the Itremo group using the combination of maximum likelihood classification, petrographic analysis, and structural data. Supervised classification successfully delineated distinct magmatic formations within the Imorona-Itsindro suite, revealing their spatial distribution and compositional heterogeneity. Petrographic observations from thin sections corroborated these units by revealing distinctive mineralogical features. Structural analyses further demonstrated a transpressional tectonic regime, characterized by ENE-WSW shortening and WNW-ESE trending strike-slip faults and associated shear zones. These structures accommodated strain through a combination of horizontal shortening and lateral movement, suggesting syn-magmatic deformation influenced by regional tectonics during the final stage of the amalgamation of Gondwana.

**Keywords:** Madagascar; Ambatofinandrahana; Imorona-Itsindro suite; Remote sensing; Structural analysis; Mapping; Lithologies

Digital Object Identifier (DOI): https://doi.org/10.5281/zenodo.17569338

Published in: Volume 4 Issue 6



This work is licensed under a <u>Creative Commons Attribution-NonCommercial-NoDerivatives 4.0 International</u> License

#### 1. Introduction

The geological history of Madagascar is characterized by a series of tectonic events and the intrusions of numerous plutons. Among these plutons, the Imorona-Itsindro suite intruded throughout all of the Precambrian domains in the center of Madagascar, such as the Antananarivo domain, the Ikalamavony domain and the Itremo group during the Proterozoic era. This suite crosscuts also the Anosyan domain in the south and the Masora domain in the east. The Imorona-Itsindro suite forms a plutons of gabbroic

and granitoid rocks (Tucker et al., 2012; Archibald et al., 2016). The gabbroic rocks consist of gabbro, diorite and norite while the granitoid rocks consists of syenite, monzonite, alkaline to sub-alkaline granite. The Ambatofinandrahana district is recognised by its mineral resources enrichment, such as rare earth elements (Rasoamalala et al., 2014), copper and galena (Andriamamonjy et al., 2018), lithium and quartz. Most of these mineralizations are related to this suite. However, there is a lack of litho-structural and characterization data of the Imorona-Itsindro suite in this district, where it intruded the Itremo group. In this paper, We applied the supervised classification technique on geological formations to understand the structural control on the Imorona-Itsindro suite emplacement and its spatial distribution. In addition, thin section technique has been used to analyze rock samples collected during field work.

#### 2. Geological setting

The Precambrian basement of Madagascar is subdivided in six domains (Tucker et al., 2012) namely from the north to the south, Bemarivo, Antananarivo, Ikalamavony, Antongil-Masora, Anosyan-Androyan and Vohibory. The study area is underlain by Itremo group within Antananarivo domain. The Itremo group is located in the west-central part of Madagascar (Figure 1a). It is mainly composed of metasedimentary rocks intercalated with orthogneiss and intruded by a younger Imorona-Itsindro suite (Tucker et al., 2007). The metamorphic grade typically increases westward from greenschist facies to amphibolite facies. The lower-grade sequence of stratified rocks in the east, initially referred to as the Schisto-Quartzo-Calcaire sequences (SQC) (Besairie, 1964), was subsequently reclassified as the Itremo Group or Schisto-Quartzo-Dolomitic sequences (SQD) (Moine, 1974). Analyses of detrital zircons from the Paleoproterozoic and Neoarchean eras suggest that these rocks were likely deposited during the Paleoproterozoic era, aged approximately 1700 to 1500 Ma (Cox et al., 1998). The Imorona-Itsindro suite intruded the Itremo group in the Ambatofinandrahana district (Figure 1b). The intrusions of Imorona consist of granitoids, while the Itsindro intrusions are mainly gabbroic rocks (Archibald et al., 2016). In addition, this suite is also subdivided in 4 sub-suites: Imorona, Itsindro, Brickaville and Ambodilafa, which intruded the Antananarivo domain including the Itremo group (Tucker et al., 2012). Recent study of the Imorona-Itsindro suite age shows a continuous magmatism between 850 and 750 Ma (Archibald et al., 2016). The emplacement of the Imorona Itsindro suite caused regional deformation within Itremo group (GAF-BGR, 2008). During this time, regional metamorphism reached temperatures of 550°C and pressures of 7.5 kbar, followed by rapid exhumation and a reduction in pressure to 4 kbar during the magmatic activity of Imorona-Itsindro (GAF-BGR, 2008).

In the study area, from the east to the west, this suite consists of the Midongy migmatitic granite, leptynitic orthogneiss, gabbro-diorite and norite, Antoetra alkaline granite, amphibole alkaliorthogneiss, amphibole granitic gneiss, and the Imorona porphyry facies.

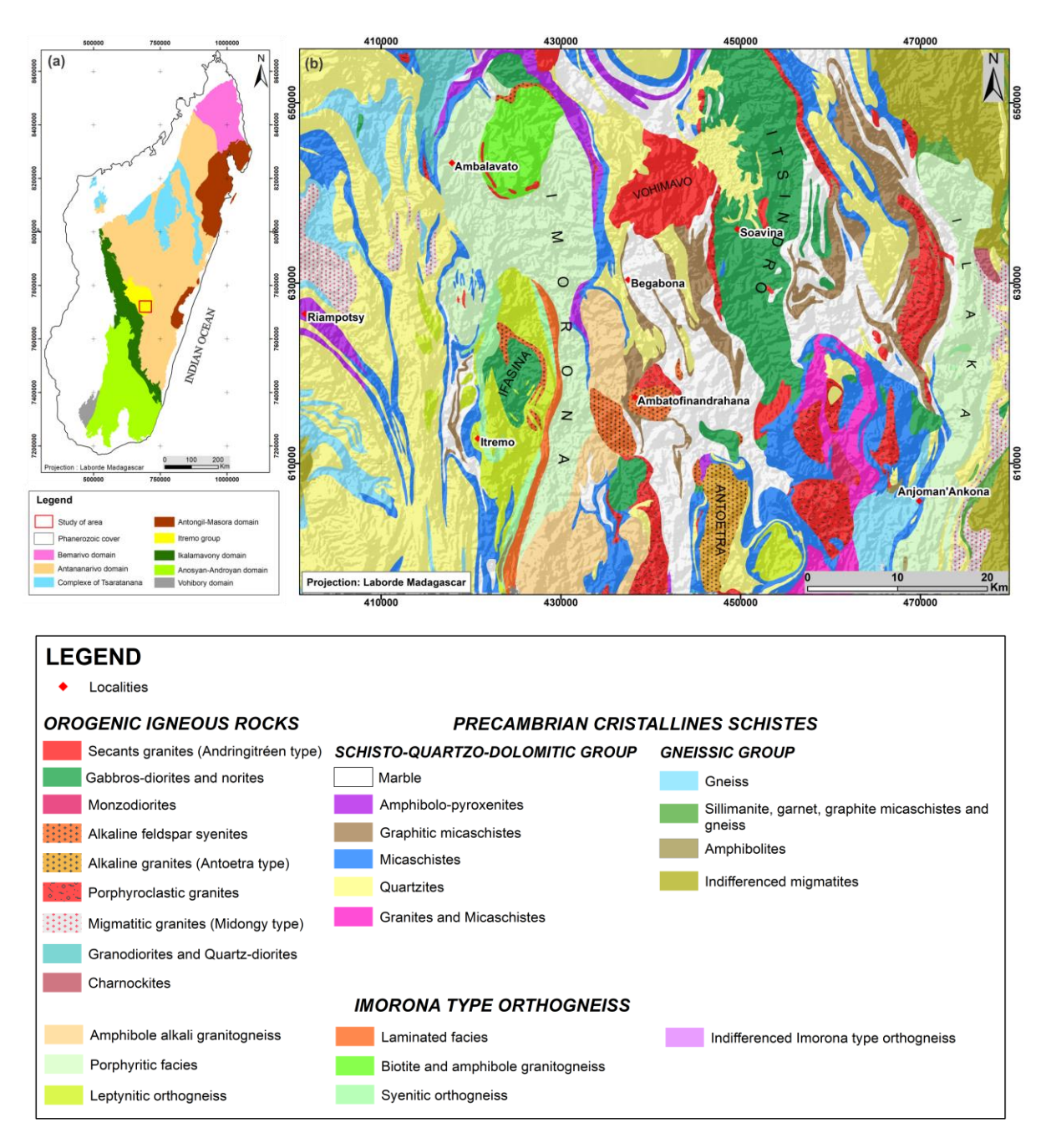


**Figure 1**. Geological and structural map of the study area: (a) Tectono-metamorphic map of Madagascar; (b) Geological map of the study area.

#### 3. Methodology

#### 3.1 Remote sensing

Nowadays, remote sensing is very helpful in mapping the geomorphology, structure and lithology. Remote sensing is a key method of modern geological mapping. It helps analyze geological structures within large area with high precision. The landsat image LC81590742014259LGN00 has been downloaded from <a href="https://earthexplorer.usgs.gov/">https://earthexplorer.usgs.gov/</a> and used in this work. In this study, we used the color composite image (RGB: 742-743) to identify the different geological structures in the Ambatofinandrahana district. These color composite images were selected based on the band

correlation. The band OLI 7 has been used and displayed as Red (R) because it shows a better reflectivity from rocks. Based on the correlation matrix between band OLI 7 and others bands, the band OLI 4 has been assigned to Green (G) and bands OLI 2 and OLI 3 assigned to Blue (B) (Razananirina and Rakontondrazafy, 2022).

To mitigate vegetation interference, a masking technique based on the Normalized Difference Vegetation Index (NDVI) was used. NDVI, a spectral vegetation index, computes the contrast in reflectance between red and near-infrared (NIR) bands, where higher values correlate with dense vegetation. By applying a defined threshold to NDVI values, vegetated regions are identified and excluded from the dataset. This process enhances the clarity of non-vegetated areas, such as exposed soil or bedrock, enabling more accurate analysis of land features.

Threshold = 
$$\mu_{NDVI}$$
 +  $(n \times \sigma_{NDVI})$ 

Where  $\mu_{NDVI}$  is the mean NDVI value of the image,  $\sigma_{NDVI}$ : standard deviation of NDVI values, n: multiplier defining how many standard deviations above the mean to set the threshold (e.g., n=1,2,3).

For this study, a threshold of n=1.5 standard deviations above the mean NDVI value were applied to isolate vegetation pixels, dynamically adapting to the statistical distribution of the dataset. This masking approach is essential in studies of Imorona-Itsindro lithology, as it helps remove the influence of vegetation on spectral signatures in the eastern part of the study area, thereby improving the result of the geological formations classification.

A supervised classification technique, using maximum likelihood algorithm, was applied to determine the spatial distribution of the Imorona-Itsindro suite. These techniques were used to map rocks based on their spectral signatures and statistical separability, thus, enhancing the accuracy of geological map. Supervised classification serves as the primary method for systematic analysis of image data. This approach relies on applying statistical algorithms to categorize image pixels into predefined rocks and soils classes based on spectral signatures (Richards, 2022). It is based on the idea of assigning each pixel in an image to the class  $\omega_i$  with the highest likelihood, given the observed data. The method assumes that the probability distribution of each class can be described by a parametric model, typically a Gaussian (Normal) distribution and selects the class maximizing the likelihood  $p(x|\omega_i)$ . The probability  $p(\omega_i|x)$  represents the likelihood that class  $\omega_i$  is the correct label for a pixel located at position x in the spectral feature space. Each class  $\omega_i$  is modeled as a multivariate normal distribution:

$$p(x|\omega_i) = \frac{1}{(2\pi)^{\frac{d}{2}} |\sum_i|^{\frac{1}{2}}} exp\left[ -\frac{1}{2} (x - \mu_i)^T \sum_i^{-1} (x - \mu_i) \right]$$

Where x = pixel vector,  $\mu_i = mean of class \omega_i$ ,  $\Sigma i = covariance matrix.$ 

Supervised classification framework was set up with 17 distinct classes and a spatial filter mask adjusted at n=1.5.

#### 3.2 Field work

Petrographical description of the rock outcrop and hand specimen observation was used to determine the type and characteristics of the geological formation. The field works help measure the attitude of foliations and lineations of some metamorphic rocks. For this study, gabbro, amphibole granitic gneiss and granite samples have been collected.

#### 3.3 Thin section

Thin sections of gabbro and granite were realized at the University of Antananarivo, Madagascar whereas the scanning image was performed for the amphibole granitic gneiss. Detailed petrography

observation was undertaken using the optical microscope. The work includes mineral identification and interpretation of the mineral texture. Photographs of thin sections were taken to provide evidence of textural relations of the various lithologies.

#### 3.4 Structural analysis

The structural analysis began with the systematic extraction of structural measurements from a 1/200 000 geological map (Moine, 1968), and 1/100 000 geological Sheet MN51 of the study area, including data such as the strike, dip of faults and foliations. These measurements, recorded as azimuths and dips for planar structures, were organized into a digital spreadsheet (CSV) to simplify further processing and providing an opportunity to unravel the tectonic history of the Ambatofinandrahana district and therefore to better understand Pan-African tectonic events in the Itremo group.

Once prepared, the data were imported into Stereonet software for detailed structural analysis. Stereographic projection serves as a critical tool in structural geology, enabling the visualization of 3D orientations on a 2D surface. Two primary methods are employed: the equal-angle (Wulff) and equal-area (Schmidt) projections. The equal-angle approach maintains angular accuracy, which is ideal for measuring angles between features, while the equal-area method preserves proportional areas, necessary for density-based studies. When projecting a line defined by its azimuth  $(\theta)$  and plunge  $(\emptyset)$ ,

the radial distance (r) from the stereonet's center varies according to the technique. For equal-angle projection, the formula  $r = R \cdot \tan\left(\frac{90^\circ - \emptyset}{2}\right)$  applies, whereas equal-area projection

uses  $r = R \cdot \sqrt{2} \cdot \sin\left(\frac{90^{\circ} - \emptyset}{2}\right)$ , where R is the stereonet's radius. These distances are converted to

Cartesian coordinates via  $x = r \cdot \cos(\theta)$  and  $y = r \cdot \sin(\theta)$ . Herein, the equal-area projection was applied. In addition, density contouring diagrams were generated to highlight dominant orientation clusters, and statistical calculations including mean orientation vectors and confidence intervals were applied to significant clusters. Finally, rose diagrams, and interpretative maps were combined to

visualize structural patterns and reconstruct the deformation history of the study area.

#### 4. Results

#### 4.1 Classification data

Among supervised classification algorithms, maximum likelihood has given the best result of the geological formations mapping.

Compared to the earlier map by Moine on 1968 (Moine, 1968), the rocks of the SQD sequences are easily distinguished from other lithologies (Figure 2a). However, the classification reveals some changes in the boundaries of some Imorona-Itsindro intrusions. Two classes are dominant namely the gabbro in blue color and the orthogneiss in green color (Figure 2b). In spite of the fact that the map scale 1/1 000 000 does not differentiate rocks by lithology within Imorona sub-suite, the used technique allowed to distinguish rock varieties at that level as secant granite, alkaline granite, porphyroclastic granite, migmatitic granite and granodiorite. The presence of white coloration, which is attributed to the marble, in the southern part of the Itsindro gabbroic rocks, may result from the chemical exchange between these two formations during the emplacement of these gabbros. The same chemical exchange is also observed in the Imorona porphyritic facies which is intruded by the biotite and amphibole granitic gneiss (Figure 2b). In addition, the amphibole alkaline granitic gneiss unit is assigned to the Imorona porphyritic facies class, suggesting lithological or compositional overlap.

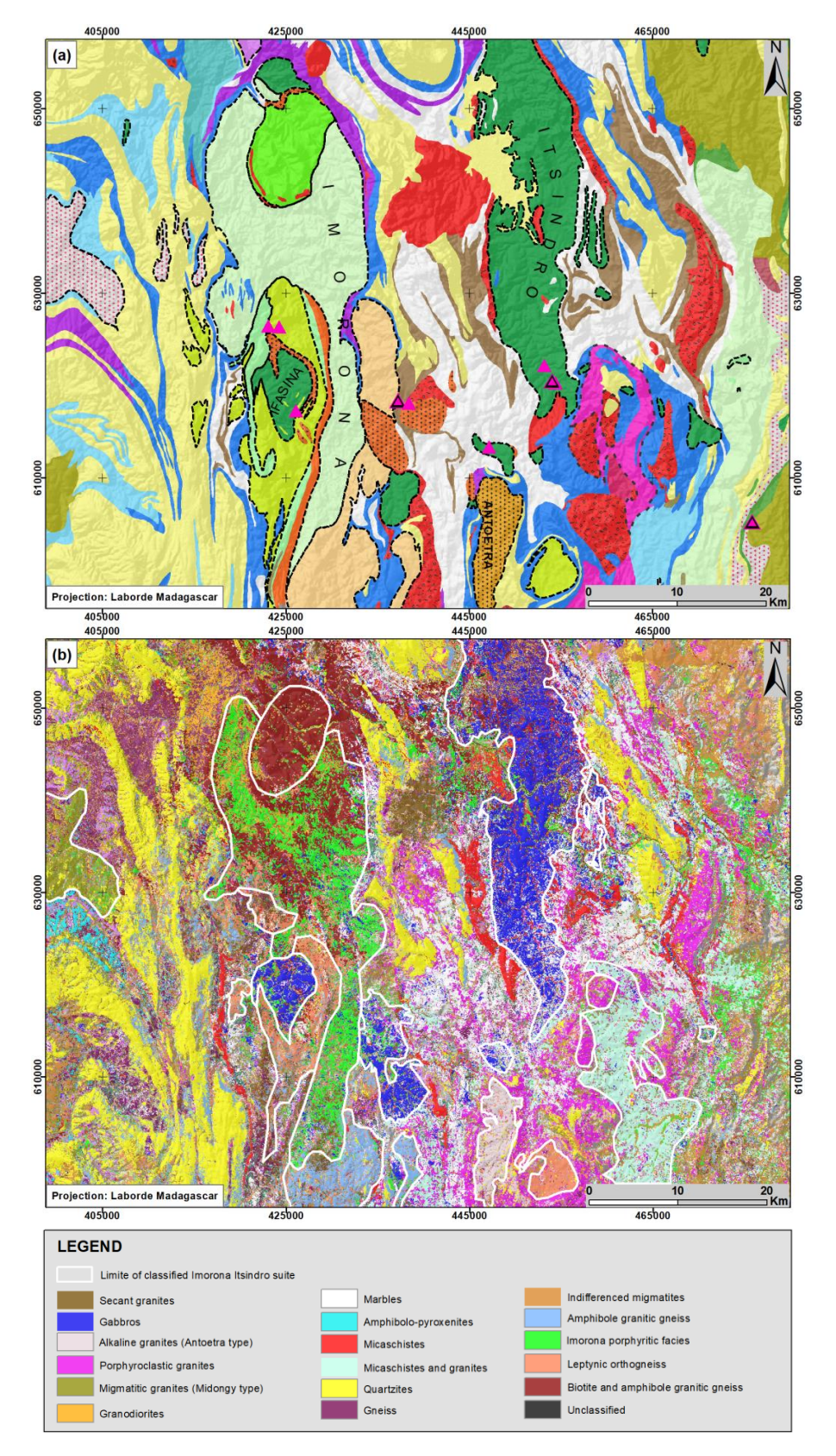


**Figure 2**. Maps showing boundaries of the Imorona-Itsindro suite in the study area **(a)** Geological map of the Ambatofinandrahana district (Same legend as in figure 1), **(b)** Geological map resulting from classification.

#### 4.2 Petrography

Samples of gabbros, amphibole granitic gneiss and granites were collected from the study area for the petrography description and thin section (Figure 3). The gabbro of Itsindro, the alkaline granite (Antoetra type) and the Imorona porphyritic facies occur as a large elongated intrusion in the Ambatofinandrahana district (Figure 3). These granitoid and gabbroic rocks have intruded into metasedimentary sequences consisting of schist, quartzite and dolomitic marble (Handke, 2001; Moine, 1974).

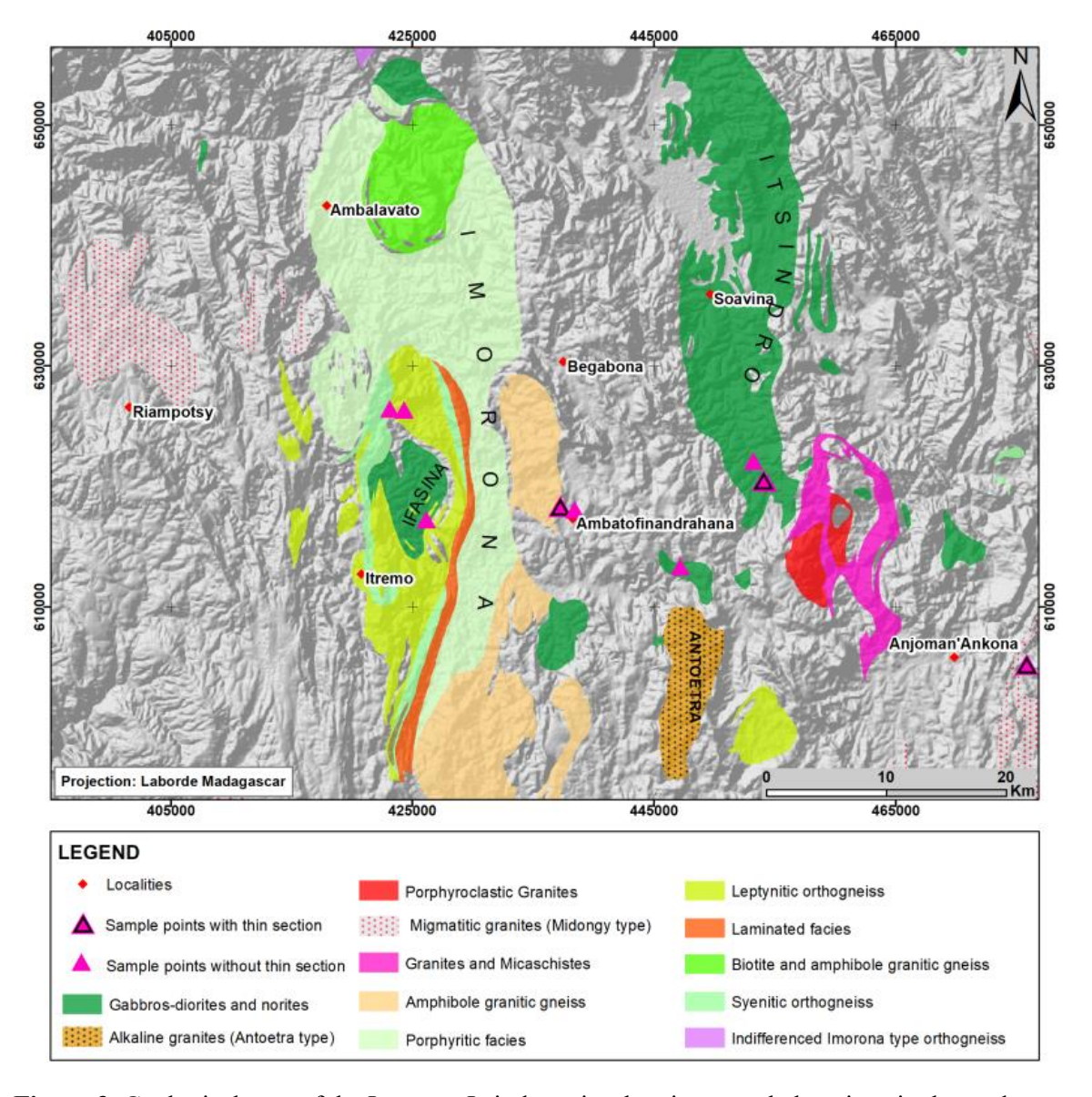
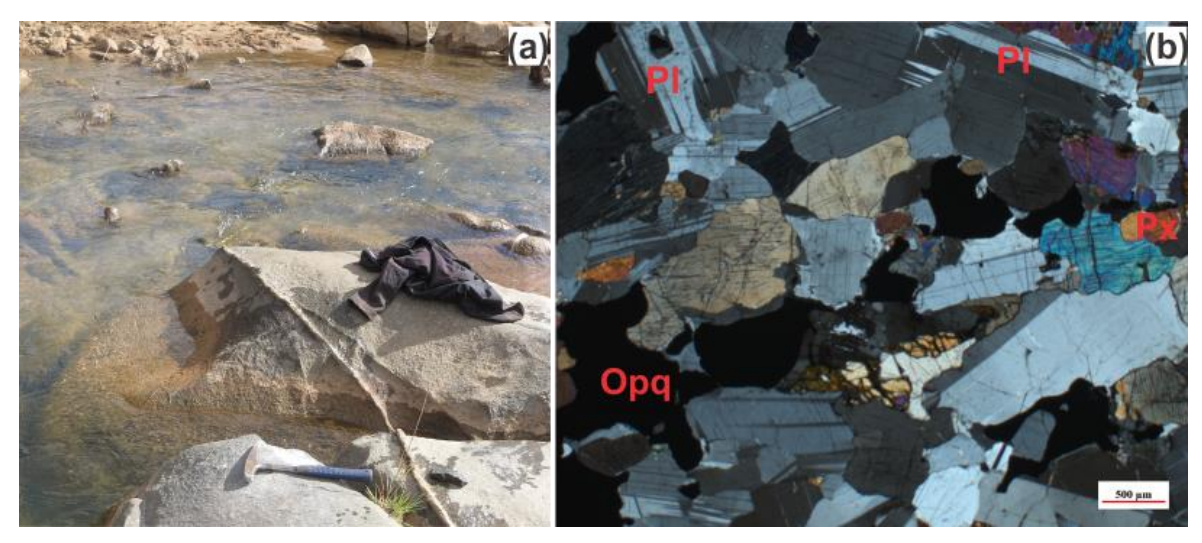


Figure 3. Geological map of the Imorona-Itsindro suite showing sample locations in the study area.

#### 4.1.1. Gabbro-diorite-norite

The samples of gabbros were collected from the Itsindro massif in the eastern part of the study area (Figure 3). They are commonly melanocrate in color and display massive, medium-grained textures (Figure 4a). In thin section, they are composed of plagioclase (70%), pyroxene (20%), hornblende (5%) and opaque minerals (5%) (Figure 4b). Plagioclase and pyroxene are the dominant mineral phase and occur as subhedral to anhedral grains (Figure 4b).



**Figure 4**. Field photo and photomicrograph of Itsindro gabbro (X= 454,215; Y= 620,165) (m) **(a)** Outcrop of the Itsindro gabbro **(b)** Microphotograph of the Itsindro gabbro. Pl: plagioclase, Px: pyroxene, Opq: opaque minerals.

#### 4.1.2. Amphibole granitic gneiss

Amphibole granitic gneiss occurs in the north-western part of Ambatofinandrahana city and exhibits weakly foliated texture (Figure 5a). They are commonly light gray and consist mainly of feldspar (40%), quartz (30%), amphibole (15%) and pyroxene (15%) (Figure 5b). Amphiboles are subhedral and mark the foliation of the rock. Plagioclases and orthose are anhedral and form the dominant minerals of the matrix.



**Figure 5**. Field photo and scanning image of amphibole granitic gneiss (X= 437,341; Y= 617,910) (m) (a) Outcrop of the amphibole granitic gneiss (b) Scanning image of the amphibole granitic gneiss Qz: quartz, Am: amphibole, Px: pyroxene.

#### 4.1.3. Migmatitic granite (Midongy type)

Granite migmatitic rocks occur in the eastern, central and western parts of the study area (Figure 6a) and display medium-grained texture. They are mesocrate in color. The Midongy migmatitic granite are slightly foliated and are composed of abundant quartz (60%), orthoclase (15%), microcline (5%) and

amphibole (5%). Accessory minerals include zircon and opaque minerals (5%). Quartz occurs as anhedral and interstitial grains and forms the most abundant mineral (Figure 6b). Plagioclase occurs as subhedral and displays a polysynthetic twinning (Figure 6b).

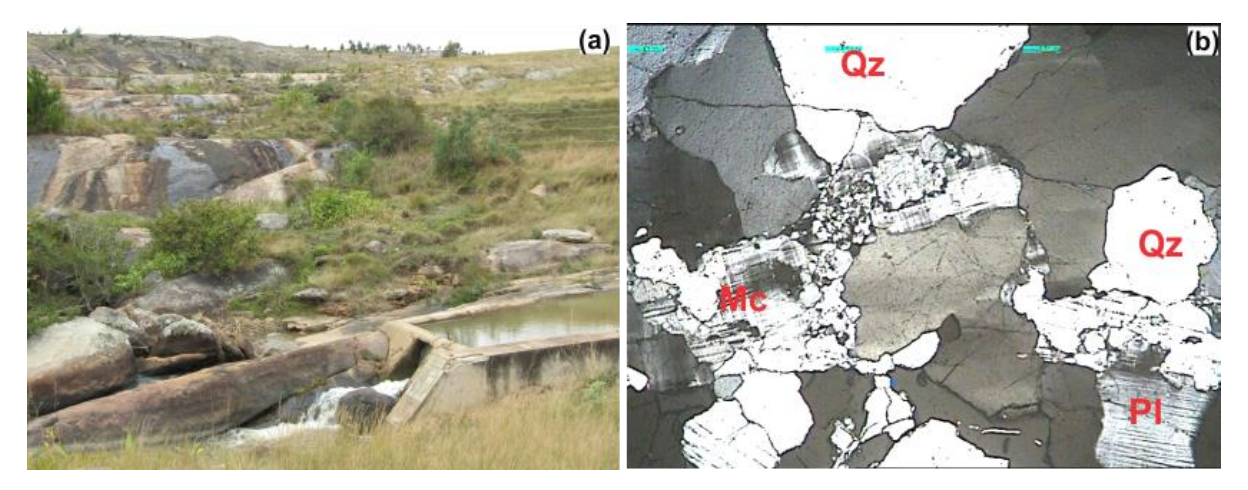


Figure 6. Field photo and photomicrograph of Midongy migmatitic granite (X= 475,935; Y= 605,129) (m) (a) Outcrop of the migmatitic granite (b) Microphotograph of the migmatitic granite Qz: quartz, Pl: plagioclase, Mc: microcline.

#### 4.3 Structural data

The analysis of satellite images revealed the presence of faults generally oriented WNW-ESE (Figure 7). The predominant WNW-ESE fault orientation is in line with the regional tectonic deformation patterns, suggesting a possible ENE-WSW orientation of compressive stress regime that shaped the geological setting of the Ambatofinandrahana region.

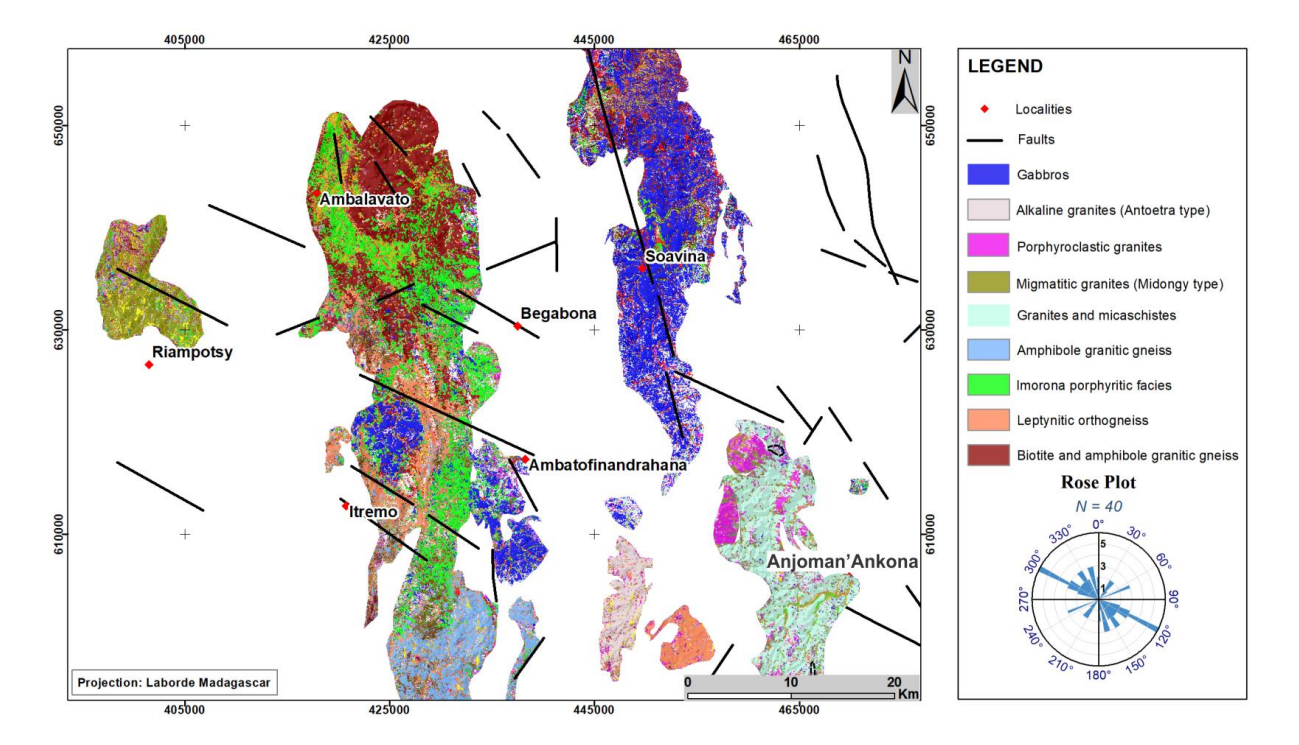
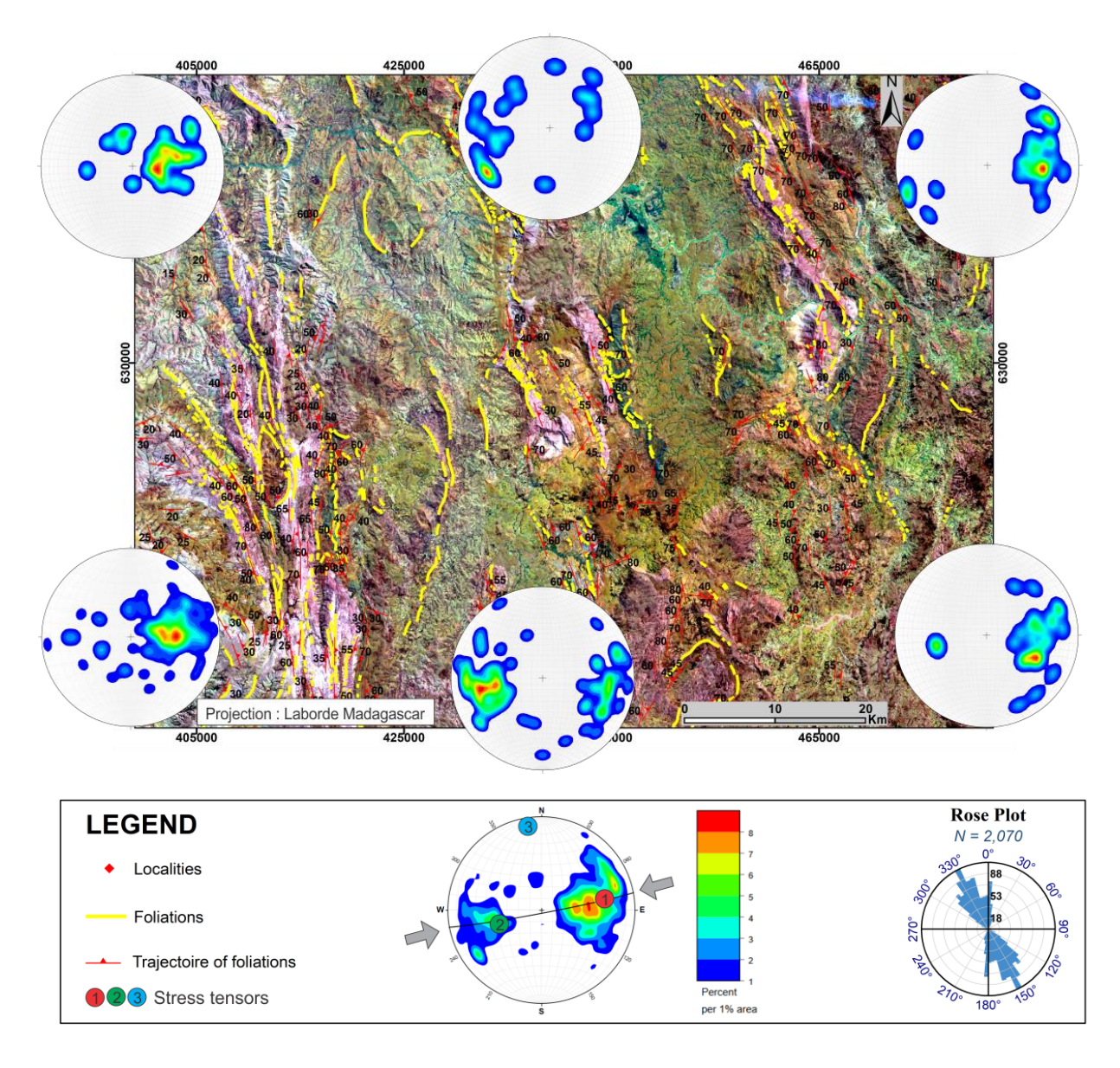


Figure 7. Structural map showing the main fault direction and the Imorona-Itsindro suite.

The contours of pole distribution were plotted using a  $1\sigma$  contour interval, revealing significant clustering of the data. The counting area represents 2.85% of the total projection surface, with an expected average of 8.74 points per zone. The statistical significance level was set at  $3\sigma$ , highlighting concentrations that deviate from a standard distribution.

Bingham analysis of the Ambatofinandrahana district shows a triaxial deformation regime, with the principal axes oriented as follows (Figure 8):

- σ<sub>1</sub> axis highlighting the maximum compression: direction 70.8°, plunge 40.6°, eigenvalue 0.6045, with a 95% confidence interval ranging from 3.4° to 6.5°, indicating oblique compression and therefore transpressive regime (Figure 9).
- σ<sub>2</sub> axis (intermediate): direction 256.0°, plunge 49.3°, eigenvalue 0.2890.
- σ<sub>3</sub> axis (maximum extension): direction 349.3°, plunge 2.9°, eigenvalue 0.1064, with a 95% confidence interval of 3.5° to 6.9°.



**Figure 8**. Structural map showing the attitude of foliations and the stereographic equal area projection displaying the density contours in the study area.

The best-fit great circle to the pole distribution has a strike of 079.3° and a dip of 87.1°, indicating a well-defined subvertical plane (Figure 8).

The rose diagram reveals a dominant orientation between  $071^{\circ}$  and  $080^{\circ}$ , accounting for 12.7% of occurrences. The mean vector associated with this distribution trends  $083.6^{\circ} \pm 6.0^{\circ}$ , with a vector length of 0.3739, showing moderate dispersion. The circular variance is 0.6261, and the concentration parameter (kappa) is 0.7973.

Finally, the Fisher mean, calculated from 307 poles, gives a mean orientation of 083.0° / 67.1°, with confidence intervals of 5.7° and 7.1°. The mean vector length is 0.6652, and the kappa (k) value is 3.0, highlighting a relatively well-defined mean orientation with a certain degree of dispersion.

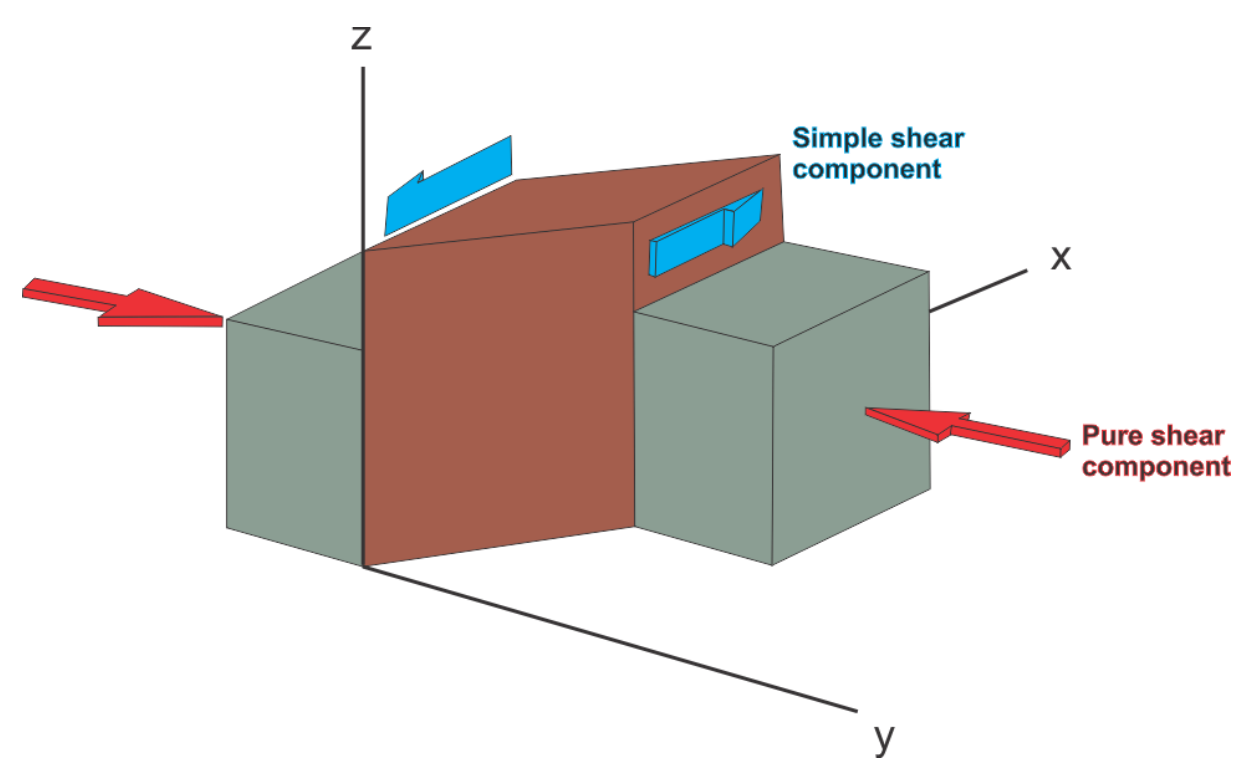


**Figure 9**. Model of transpression illustrating the pure shear and simple shear components (modified from Fossen, 2016; Sanderson and Marchini, 1984).

#### 5. Discussion

The analysis of satellite images using color composite images and supervised classification techniques allowed to map the Imorona-Itsindro suite in the Ambatofinandrahana district. A new refined geological outline of the suite was obtained, with particular emphasis on the lithology spatial distribution and structure identification. The newly delineated lithological boundaries are more accurate and show more details comparatively with the earlier map. The result shows the satellite image analysis relevance in geological mapping of areas with limited access. The structural analysis has unveiled a ENE-WSW transpressional stress regime, characterized by oblique compressional forces, as demonstrated by the principal stress axis ( $\sigma_1$ ). The near-vertical alignment of the minimum stress axis ( $\sigma_3$ ) and the steeply inclined fault plane (strike = 079.3°, dip = 87.1°) corroborate transpressive deformation, integrating crustal shortening and lateral strike-slip movement. Transpression refers to a tectonic process where horizontal shearing (strike-slip movement) occurs parallel to a geological structure, while compressional forces occur simultaneously perpendicular to it, resulting in combined deformation (Figure 9). The interaction between strike slip motion and crustal

shortening often gives complex structural features within the Earth's crust (Fossen, 2016; Sanderson and Marchini, 1984). East-west horizontal shortening in a transpressive regime occurred in the northern and southern parts of Madagascar and is likely linked to the D2 deformation event (Goncalves et al., 2003; J. E. Martelat et al., 1999). Tucker (2007) also noted the presence of this transpressive regime within the Itremo Group but did not provide further details on the tectonic stresses responsible for the deformation. In Ambatofinandrahana district, the WNW-ESE trending faults and shear zones (Figure 7), indicate the transpressional tectonic environment caused by ENE-WSW oblique compression. Faults are perpendicular to  $\sigma_3$  and parallel to  $\sigma_1$ , facilitating both ENE-WSW crustal compression and lateral strike-slip movement. We suggest that the WNW-ESE trending faults and shear zones in the study area are not directly related to the D2 deformation phase but are instead associated with ENE-WSW shortening within a sinistral transpressive regime. However, the precise timing of this ENE-WSW oriented shortening remains unresolved.

The occurrences of asymmetric kinematic structures and consistent shear sense indicators demonstrate that simple shear is the dominant deformation mechanism in the study area. In addition, this structure indicates syn-magmatic deformation in relation with the regional tectonics during the final stage of the amalgamation of Gondwana. The Bongolava-Ranotsara shear zone dominated by simple shear (Martelat et al., 2000) and the virgation of Antananarivo (Goncalves et al., 2003; Nédélec et al., 2000) are likely the limit of this ENE-WSW transpressive regime to the south and north respectively.

#### 6. Conclusion

The combined application of supervised classification, petrographic studies and structural analysis has provided a robust framework for understanding the magmatic evolution and tectonic history of the Imorona-Itsindro suite in the Ambatofinandrahana district. The supervised classification not only did delineate Imorona-Itsindro suite, but also gave its spatial distribution and differentiation by lithology. Petrographic observations from thin sections further corroborated these classifications by revealing critical mineralogical signatures, such as variations in feldspar composition, mafic mineral assemblages and textural features.

For the structural analysis, the regime is characterized by ENE-WSW transpression, as evidenced by the development of WNW-ESE trending strike-slip faults and associated shear zones. These structures likely accommodated regional strain through a combination of horizontal shortening and lateral displacement, characteristic of transpressive regime. The relationship between magmatic processes and transpressional tectonics indicates that the timing and location of magma emplacement were controlled by shear zones associated with subduction, probably during the amalgamation of Gondwana. Future studies could enhance these results by integrating geochronological data to constrain the timing of magmatic events relative to deformation phases, and by employing 3D structural modeling to better resolve the geometry of shear zones and their role in magma transport.

#### Reference

- [1] Andriamamonjy, A., Andrianaivo, L., Razafimahatratra, D., & Andriamifidisoa, M. (n.d.). CARACTERISTIQUES DU GITE DE GALENE D'AMBATOFANGEHANA AMBATOFINANDRAHANA MADAGASCAR. Retrieved June 29, 2025, from http://madarevues.recherches.gov.mg/IMG/pdf/hary7 1 .pdf.
- [2] Archibald, D. B., Collins, A. S., Foden, J. D., Payne, J. L., Holden, P., Razakamanana, T., De Waele, B., Thomas, R. J., & Pitfield, P. E. (2016). Genesis of the Tonian Imorona–Itsindro magmatic Suite in central Madagascar: Insights from U–Pb, oxygen and hafnium isotopes in zircon. *Precambrian Research*, 281, 312–337. https://www.sciencedirect.com/science/article/pii/S0301926816301589.
- [3] Besairie, H. (1964). Carte géologique de Madagascar : Antananarivo. Service Géologique de Madagascar, Scale, 1(1,000,000).

- [4] Cox, R., Armstrong, R. A., & Ashwal, L. D. (1998). Sedimentology, geochronology and provenance of the Proterozoic Itremo Group, central Madagascar, and implications for pre-Gondwana palaeogeography. *Journal of the Geological Society*, 155(6), 1009–1024. https://pubs.geoscienceworld.org/jgs/article-abstract/155/6/1009/93945.
- [5] Fossen, H. (2016). *Structural geology*. Cambridge university press. https://books.google.com/books?hl=fr&lr=&id=86GzCwAAQBAJ&oi=fnd&pg=PR8&dq=Haakon+fossen&ots=gg35KEe7Vp&sig=99IH3uFTLmpKvGAHDpXLzOqAeJo.
- [6] GAF-BGR. (2008). Explanatory notes for the Ikalamavony domain, central and western Madagascar. Réalisation des travaux de cartographie géologique de Madagascar, révision approfondie de la cartographie géologique et minière aux échelles 1/100,000 et 1/500,000 zone Sud. République de Madagascar, Ministère de l'Energie et des Mines Antananarivo.
- [7] Goncalves, P., Nicollet, C., & Lardeaux, J.-M. (2003). Finite strain pattern in Andriamena unit (north-central Madagascar): Evidence for late Neoproterozoic–Cambrian thrusting during continental convergence. *Precambrian Research*, 123(2–4), 135–157. https://www.sciencedirect.com/science/article/pii/S0301926803000652.
- [8] Handke, M. J. (2001). *Neoproterozoic magmatism in the Itremo region, central Madagascar: Geochronology, geochemistry, and petrogenesis*. Washington University in St. Louis. https://search.proquest.com/openview/6f8f2966789b7fb0fd0ff8f06ba5f292/1?pq-origsite=gscholar&cbl=18750&diss=y.
- [9] Martelat, J. E., Lardeaux, J. M., Nicollet, C., & Rakotondrazafy, R. (1999). Exhumation of granulites within a transpressive regime: An example from southern Madagascar. *Gondwana Research*, 2(3), 363–367. https://www.sciencedirect.com/science/article/pii/S1342937X05702756.
- [10] Martelat, J.-E., Lardeaux, J.-M., Nicollet, C., & Rakotondrazafy, R. (2000). Strain pattern and late Precambrian deformation history in southern Madagascar. *Precambrian Research*, 102(1–2), 1–20. https://www.sciencedirect.com/science/article/pii/S0301926899000832.
- [11] Moine, B. (1968). Carte du massif schisto-quartzo-dolomitique, region d'Ambatofinandrahana, centreouest du socle cristallin précambrien de Madagascar. *Centre de l'Institut Géographique National à Tananarive (Imprimeur), Sciences de La Terre, Nancy (Editeur), Scale, 1*(200,000).
- [12] Moine, B. (1974). CARACTERES DE SEDIMENTATION ET DE METAMORPHISME DES SERIES PRECAMBRIENNES EPIZONALES A CATAZONALES DU CENTRE DE MADAGASCAR (REGION D'AMBATOFINANDRAHANA). APPROCHE STRUCTURALE, PETROGRAPHIQUE ET SPECIALEMENT GEOCHIMIQUE. https://pascal-francis.inist.fr/vibad/index.php?action=getRecordDetail&idt=PASCALGEODEBRGM7520068103.
- [13] Nédélec, A., Ralison, B., Bouchez, J., & Grégoire, V. (2000). Structure and metamorphism of the granitic basement around Antananarivo: A key to the Pan-African history of central Madagascar and its Gondwana connections. *Tectonics*, 19(5), 997–1020. https://doi.org/10.1029/2000TC900001.
- [14] Rasoamalala, V., Salvi, S., Béziat, D., Ursule, J.-P., Cuney, M., De Parseval, P., Guillaume, D., Moine, B., & Andriamampihantona, J. (2014). Geology of bastnaesite and monazite deposits in the Ambatofinandrahana area, central part of Madagascar: An overview. *Journal of African Earth Sciences*, 94, 128–140. https://www.sciencedirect.com/science/article/pii/S1464343X13002185.
- [15] Razananirina, H.D., and Rakotondrazafy, R. (2022). Airborne Magnetic Survey and Remote Sensing Applied to Structural Study in Vohilava Area Madagascar. *International Journal of Geography and Geology*, 11(2), 43–61. https://ideas.repec.org/a/pkp/ijogag/v11y2022i2p43-61id3165.html.
- [16] Richards, J. A. (2022). *Remote Sensing Digital Image Analysis*. Springer International Publishing. https://doi.org/10.1007/978-3-030-82327-6.
- [17] Sanderson, D. J., and Marchini, W. R. D. (1984). Transpression. *Journal of Structural Geology*, 6(5), 449–458. https://www.sciencedirect.com/science/article/pii/0191814184900580.
- [18] Tucker, R. D., Kusky, T. M., Buchwaldt, R., & Handke, M. J. (2007). Neoproterozoic nappes and superposed folding of the Itremo Group, west-central Madagascar. *Gondwana Research*, 12(4), 356–379. https://www.sciencedirect.com/science/article/pii/S1342937X06002954
- [19] Tucker, R. D., Peters, S. G., Roig, J. Y., Théveniaut, H., & Delor, C. (2012). Cartes Géologique et Métallogéniques de la République de Madagascar à 1/1000000. *United States Geological Survey: Reston, VA, USA*, 1–257.